AD-A208 100

OFFICE OF NAVAL RESEARCH

Contract: N00014-85-K-0222

Work Unit: 4327-555

Scientific Officer: Dr. Richard S. Miller

Technical Report No. 18

PULL-OUT AND PUSH-OUT ·ıS FOR RUBBER-TO-METAL ADHESION

by

A. N. Gent and S. Y. Kaang

Institute of Polymer Science
The University of Akron
Akron, Ohio 44325

May, 1989

067

SECURITY CLASSIFICATION OF THIS PAGE (When Data Entered)

REPORT DOCUMENTATION PAGE

READ INSTRUCTIONS BEFORE COMPLETING FORM

1. REPORT NUMBER Technical Report No. 18	2. GOVT ACCESSION NO.	3. RECIPIENT'S CATALOG NUMBER
4. TITLE (and Subtitle) Pull-out and Push-out Tests for Rubber-to-Metal Adhesion		5. TYPE OF REPORT & PERIOD COVERED Technical Report
		6. PERFORMING ORG. REPORT NUMBER
7. AUTHOR(s) A. N. Gent and S. Y. Kaang		8. CONTRACT OR GRANT NUMBER(s) N00014-85-K-0222
9. PERFORMING ORGANIZATION NAME AND ADDRESS Institute of Polymer Science The University of Akron Akron, OH 44325		10. PROGRAM ELEMENT, PROJECT, TASK AREA & WORK UNIT NUMBERS 4327-555
11. CONTROLLING OFFICE NAME AND ADDRESS Office of Naval Research Power Program Arlington, VA 22217-5000		12. REPORT DATE May 1989
		13. NUMBER OF PAGES 26
14. MONITORING AGENCY NAME & ADDRESS (if different from Controlling Office)		15. SECURITY CLASS. (of this report) Unclassified
		15a. DECLASSIFICATION/DOWNGRADING SCHEDULE

16. DISTRIBUTION STATEMENT (of this Report)

According to attached distribution list.
Approved for public release; distribution unrestricted.

17. DISTRIBUTION STATEMENT (of the abstract entered in Block 20, if different from Report)

18. SUPPLEMENTARY NOTES

Submitted for publication in: Surface Science

19. KEY WORDS (Continue on reverse side if necessary and identify by block number)

Adhesion, Bonding, Compression, Debonding, Failure, Fracture, Friction, Rubber, Steel, Tension.

20. ABSTRACT (Continue on reverse side if necessary and identify by block number)

A steel rod embedded in a rubber block can be debonded either by pulling it out or by pushing it out. A comparison is made between the two failure forces. It is shown that friction, aggravated by the tendency of rubber to undergo Poissonian contraction as the block is stretched, makes the pull-out

DD FORM 1 JAN 73 1473 EDITION OF 1 NOV 65 IS OBSOLETE
S/N 0102-LF-014-6601

SECURITY CLASSIFICATION OF THIS PAGE (When Data Entered) force much higher for rods of large diameter, deeply embedded in the block. On the other hand, the push-out experiment is difficult to carry out because of the inherent instability of tall blocks in compression. Thus, pull-out is still the preferred way of measuring adhesion, but the product aL, where a is the rod radius and L the depth of embedment, should be made much smaller than the cross-sectional area of the block in order to minimize frictional contributions to the failure force.

1. Introduction

A pull-out test for adhesion has many advantages. In its simplest form, an inextensible rod, cord or fiber is partially embedded in a long elastic block, and the force required to pull the rod out of the block is measured, Figure 1. A debond propagates up the rod, starting at its embedded end. The pull-out force is directly related to the work of breaking the interfacial bond and the work of stretching the block as it becomes detached. If the elastic properties of the block are known, the fracture work per unit area of interface can be calculated (1). Moreover, because the work of fracture is greater for fracture surfaces of greater radius, there is a natural tendency for the failure to remain as close to the interface as possible. Thus, the mechanics of fracture drive the locus of failure towards the interface, even when the bond is strong.

In practice, the pull-out force increases when the embedded length is long, and increases continuously as the rod is pulled out, because of friction in the already-detached portions. The additional force can be quite large. Indeed, frictional resistance to pull-out is auto-catalytic: the greater the frictional resistance to pull-out, the greater the tension in the block and the greater the tendency of the material to grip the rod by Poissonian contraction (2).

Because of this difficulty, we have carried out a study of debonding in compression, for comparison. In this case, the block expands and separates from the rod in a radial direction as it detaches from the rod and becomes compressed. Thus, the frictional component should vanish. A comparison of the two experiments should therefore clarify the role of friction in pull-out mechanics.

2. Theoretical considerations

An analysis of pull-out forces has been given previously (1,2). For growth of a debond along the rod by a distance dc, work of detachment is required, given by

$$dW_1 = 2\pi a G_a \, dc$$

where a is the rod radius. In addition, work of deformation is imparted to the newly-debonded portion of the block, given by

$$dW_2 = (F^2 / 2AE) \, dc$$

where F is the pull-out force, A is the cross-sectional area of the block and E is the tensile (Young) modulus of the block material, assumed for simplicity to be linearly elastic. Work is provided to the system by additional extension of the block, given by

$$dW = F \, e \, dc = (F^2/AE) \, dc$$

where e is the elongation of the detached portion of the block under the pull-out force F. Conservation of energy requires that

$$dW = dW_1 + dW_2.$$

Hence (1),

$$F^2 = 4\pi a A E G_a \qquad (1)$$

Work of frictional sliding can be readily taken into account for the special case of a block of circular cross-section, of radius b, where b is not much greater than the rod radius a. These assumptions allow us to calculate the pressure P exerted on the rod by the tendency of the stretched block to undergo Poissonian contraction, given by

$$P = Ee[1 - (a^2/b^2)]/3 = F/3\pi b^2$$

at a point where the tensile force in the block is $\underline{F}$. The corresponding frictional contribution $\underline{dF}$ to $\underline{F}$ is given by

$$dF = \mu P(2\pi a\ dx) = (2\mu aF/3b^2)\ dx,$$

where μ is the coefficient of friction, assuming that the local frictional stress is proportional to the local pressure. By integrating over the already debonded length of the rod, denoted $\underline{L}$, we obtain the total pull-out force as

$$\ln (F/F_o) = 2\mu aL/3b^2 \qquad (2)$$

where $\underline{F_o}$ denotes the pull-out force when $\underline{L = 0}$, i.e., in the absence of friction. $\underline{F_o}$ is given by Equation 1.

In an earlier approximate treatment of frictional contributions to pull-out (2), the frictional stress was assumed to be constant over the debonded portion of the rod. In the present analysis, it is assumed to increase from the current location of the detachment front to a maximum at the embedded end of the rod, in accord with the increasing pressure set up by increasing tension in the block. This is thought to be a better representation of the mechanics of pull-out, although it still contains a number of simplifying assumptions, notably that the frictional force at the interface acts to stretch the block uniformly, throughout the cross-section of the block. This is likely to be an unsatisfactory assumption for debonds of small length and for rods of small radius relative to the block.

It is also known that the coefficient of friction of rubber is not strictly constant. Instead, it decreases as the pressure is increased (3). The present treatment is thus only an approximate guide to the effect of friction. Nevertheless, it indicates that friction can be a major factor in pull-out experiments. Indeed, both analyses show that the pull-out force will increase rapidly as the length L of the debonded portion of the rod increases, relative to the radius b of the block in which it is embedded. Moreover, the effect of friction is multiplied by the ratio of the rod and block radii. Thus, frictional effects will be most pronounced for a rod deeply embedded within a block whose radius is not much greater than that of the rod.

In compression, on the other hand, no frictional effects are expected, because the detached portion of the block will bulge outwards, away from the rod. An experimental comparison of the two processes is made below.

2. Experimental details

Preparation of samples

Steel rods of various radii, ranging from 0.25 to 1.65 mm were cleaned with acetone and painted with thin coats of two rubber-to-metal bonding agents (Chemlok 205 and Chemlok 220, Lord Corporation). They were then placed along the central axis of a mold having a cavity of square cross-section, 12.7 x 12.7 mm, and 76 mm long. A rubber block was then molded around the rod, forming a bond with the steel during vulcanization. The mix formulation used to prepare the blocks consisted of: natural rubber, 100 parts by weight, and dicumyl peroxide, 2 parts by weight. Vulcanization was effected by heating for 50 min at 150°C. Young's modulus was determined from simple tension measurements to be 1.05 MPa.

Blocks were prepared of various lengths, from 6.5 to 75 mm. Similar blocks were prepared with a central hole in place of the bonded steel rod, the hole being slightly larger in diameter than the rod. Two blocks were placed in series as shown in Figure 2, so that on compression the rod emerged from the upper block and entered the hole in the lower block. To avoid buckling instabilities under compressive loads it was found to be necessary to employ short lower blocks (which are not reinforced by a central steel rod) when the upper block was long, and short upper blocks for rods of small diameter (which do not reinforce effectively against buckling).

Unfortunately, the elastic behavior of short blocks in compression is not well described by linear elastic relations, with Young's modulus $\underline{E}$, because of severe and increasing constraints against lateral expansion. Furthermore, these constraints are not well defined in compression against frictional surfaces, as in the present experiments. Estimates of the effective modulus of compression specimens, for use in Equation 1, were obtained from the initial slopes of experimental relations between compression force and deflection, but they must be regarded as rather approximate measures.

Blocks of larger cross-section were obtained by glueing a number of blocks together, side by side, with a rubbery adhesive (Pliobond, The

Goodyear Tire & Rubber Company). In these cases, the central block of the upper assembly contained the steel rod.

All experiments were carried out at room temperature, using a cross-head speed of 5 mm/min.

Determination of debonding force

In pull-out experiments the force rose continuously with increasing extension of the sample to reach a well-defined maximum value, taken as the pull-out force *F*. A representative relation between tensile force and deflection is shown in Figure 3. Irregularities in the curve suggest that debonding began at a relatively low force, about 40 N, but the force *F* required to pull the rod out completely was considerably greater, about 75 N. This difference is attributed to friction.

Two methods were used to determine the debonding force in compression experiments:

(i) In the first, the sample was compressed and the force-deflection relation studied. A typical result is shown in Figure 4. The force rose sharply in the initial stages, as the lower block was increasingly compressed, and then abruptly fell when debonding started at the lower end of the rod. Both the peak value, about 55 N, and the subsequent minimum value, about 40 N, have been employed as measures of failure force.

As debonding continued the force fluctuated about a gradually rising average value and eventually rose again when most of the rod had become detached. Using polarized light, progress of the debond could be observed by corresponding movement of the photoelastic stress pattern along the rod, Figure 5. It was found to propagate at substantially constant force over most of the rod length, but the upper end of the rod stayed bonded even when large compressive forces were imposed.

(ii) The amount of energy lost in a loading and unloading cycle was determined from the area between loading and unloading force-deflection relations. Expressed as a fraction of the energy put in, given by the area under the loading curve, it is denoted the mechanical hysteresis ratio $\underline{h}$. Values of $\underline{h}$ were determined for increasing levels of applied force. Up to the point at which sliding began between the rubber and rod surfaces, $\underline{h}$ was relatively small, about 10 percent, and constant, but a marked increase was evident when sliding started. This feature was also used to recognize the onset of debonding.

Typical relations between $\underline{h}$ and the maximum applied compressive force are shown in Figure 6 for strongly-bonded and weakly-bonded rods. The onset of debonding is clear, at forces of about 35 N and about 7 N, respectively. Values of push-out force determined in this way were found to be similar to those determined directly from the loading curves, lying between the initial peak force and the subsequent minimum value.

3. Experimental results and discussion

Measurements were made of pull-out and push-out forces for bonded steel rods having a wide range of diameter $\underline{d}$, embedded in rubber blocks having a wide range of cross-sectional area $\underline{A}$. The results are plotted in Figures 7 and 8 in accordance with Equation 1, i.e., as a function of $\underline{d}^{1/2}$ for blocks of constant cross-sectional area, and as a function of $\underline{A}^{1/2}$ for rods of constant diameter. The theoretical treatment, ignoring friction, predicts linear relations between failure force $\underline{F}$ and $\underline{d}^{1/2}$, and between $\underline{F}$ and $\underline{A}^{1/2}$.

Push-out measurements were in reasonable agreement with these predictions, values for both peak force and minimum force falling on linear relations passing through the origin. Pull-out forces were similar in magnitude for rods of the smallest diameter, but became considerably higher as the rod diameter increased, and deviated significantly from a linear relation through the origin, Figure 7. These discrepancies are attributed to frictional contributions to the pull-out force, which are expected to increase with increasing rod diameter, Equation 2.

It should be noted that non-linear elastic behavior of rubber would cause the opposite effect. A higher effective modulus of elasticity in compression would lead to <u>higher</u> push-out forces, rather than lower ones, Equation 1. Thus, the effect of increased stiffness in compression seems to be rather small in the present experiments; it is certainly not responsible for the lower failure forces.

As expected, pull-out forces were higher than push-out forces for rods of constant diameter embedded in blocks of different cross-sectional area, Figure 8. The relative difference became smaller, however, for blocks of greater cross-section. This is also consistent with a frictional contribution to the pull-out force, which would become less significant in blocks of large cross-section A [$\equiv \pi(b^2-a^2)$ in Equation 2]. For blocks of the largest cross-sections there were indications of departures from a linear dependence of the failure force upon $A^{1/2}$, both for pull-out and push-out experiments, Figure 8. When the block cross-section is large in comparison with the rod radius a, then the assumption of uniform extension or compression of the debonded portion of the block is probably unsatisfactory.

4. Conclusions

A study has been carried out of adhesive failure forces for a steel rod embedded in, and bonded to, a rubber block. Emphasis has been placed on comparing tension (pull-out) and compression (push-out) forces. A frictional contribution to the pull-out force appeared to be significant for rods having a diameter greater than about 0.5 mm in the present experiments. Indeed, it became a large fraction of the total force when the rod diameter was 1 mm or more. On the other hand, it was negligibly small in push-out experiments. They would therefore be preferred on this basis for measuring the strength of adhesion. But experimental difficulties in carrying out compression tests are considerable. Tall blocks become unstable under large compressive loads and short ones are markedly stiffer than long ones due to restraints on their lateral expansion which are difficult to specify and control. Thus, although measurements of push-out force for a wide variety of samples have been shown to be in good accord with a simple theoretical treatment of debonding, ignoring friction, it is recommended that pull-out tests be retained for assessing the strength of adhesive bonds.

Caution is necessary to minimize the effect of friction. The theoretical treatment indicates that the product aL of the rod radius a and the embedded length L should be held smaller than the cross-sectional area of the block in which the rod is embedded.

Acknowledgements

This work forms part of a program of research on adhesion supported by the Office of Naval Research (Contract N00014-85-K-0222; Project Officer, Dr.R.S.Miller) and by grants-in-aid from Lord Corporation and Westvaco Corporation. The authors are also indebted to Professor G.R.Hamed of these laboratories for helpful advice.

References

1. A.N.Gent, G.S.Fielding-Russell, D.I.Livingston and D.W.Nicholson, J.Mater.Sci. 16, 949 (1981).
2. A.N.Gent and O.H.Yeoh, J.Mater.Sci. 17, 1713 (1982).
3. A.Schallamach, Wear 1, 384 (1958).

Figure Legends

Figure 1. Pull-out test for adhesion between rubber and steel.

Figure 2. Push-out test for adhesion.

Figure 3. Typical relation between tensile force $\underline{F}$ and deflection of the testpiece ends for pull-out, Figure 1. Rod diameter: 1.4 mm.

Figure 4. Typical relation between compressive force $\underline{F}$ and deflection of the testpiece ends for push-out, Figure 2. Rod diameter: 2.5 mm.

Figure 5. Photoelastic stress patterns during push-out, showing progress of debonding. Compressive force: $\underline{a}$, 0 N; $\underline{b}$, 17 N; $\underline{c}$, 53 N; $\underline{d}$, 40 N; $\underline{e}$, 45 N; $\underline{f}$, 59 N. Rod diameter, 1.9 mm; block length, 50 mm (top), 6.4 mm (bottom).

Figure 6. Experimental relations between hysteresis ratio $\underline{h}$ and maximum compressive force $\underline{F}_c$ for push-out of a weakly-bonded (●) and a strongly-bonded (■) rod, of diameter 1.6 mm. Sample with no rod: ▲. Block length: 25mm (top); 25 mm (bottom); cross-sectional area, 12.7 mm x 12.7 mm.

Figure 7. Experimental relations between failure force $\underline{F}$ and diameter $\underline{d}$ of a steel rod, embedded in a rubber block of cross-section 12.7 mm x 12.7 mm. Pull-out force, ▲. Push-out forces: maximum values, ●; minimum values, ○.

Figure 8. Experimental relations between failure force $\underline{F}$ and cross-sectional area $\underline{A}$ of the block in which the steel rod was embedded. Rod diameter, 2.5 mm. Pull-out forces, ▲; push-out forces, ●.

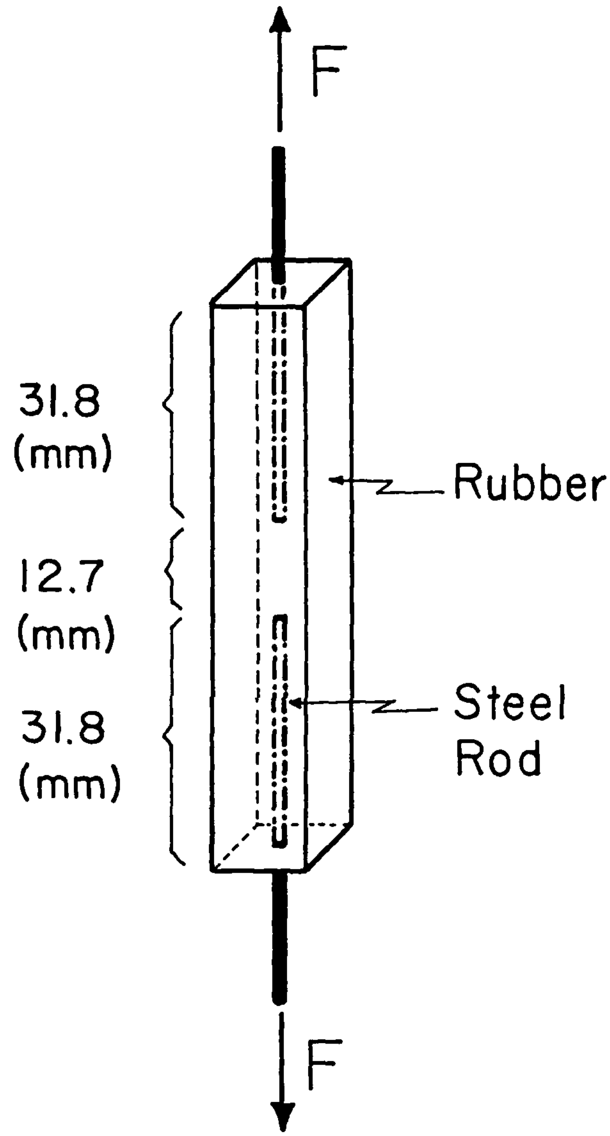

FIG. 1

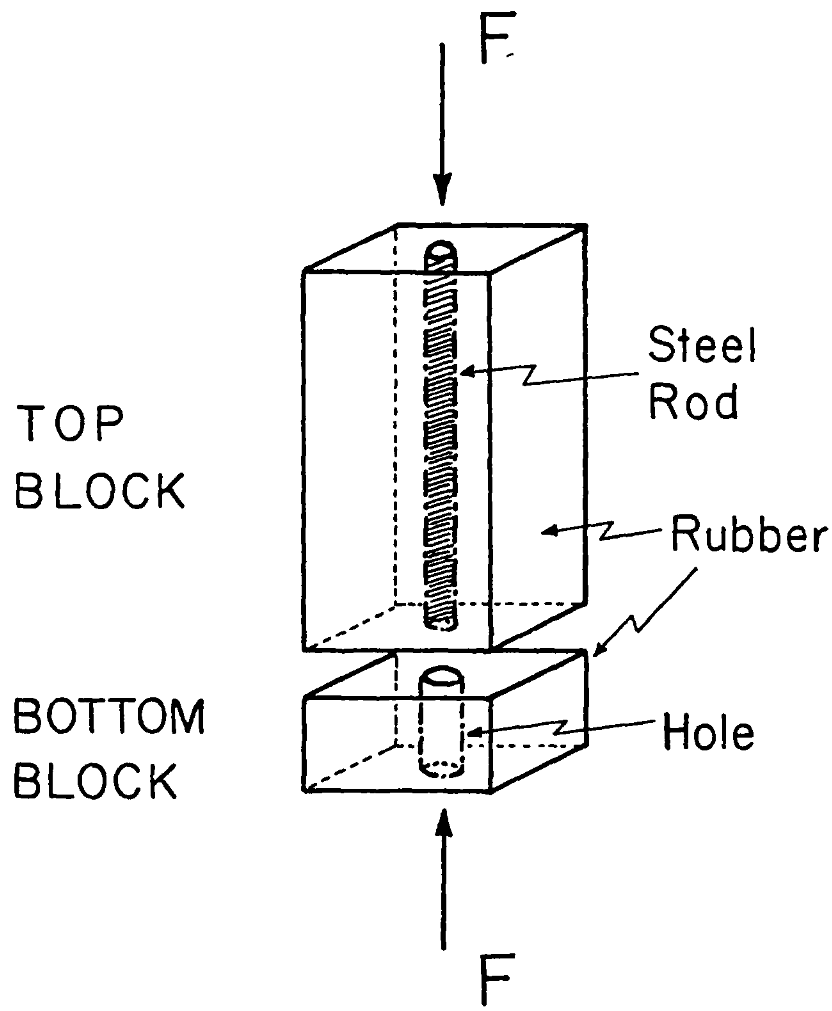

FIG. 2

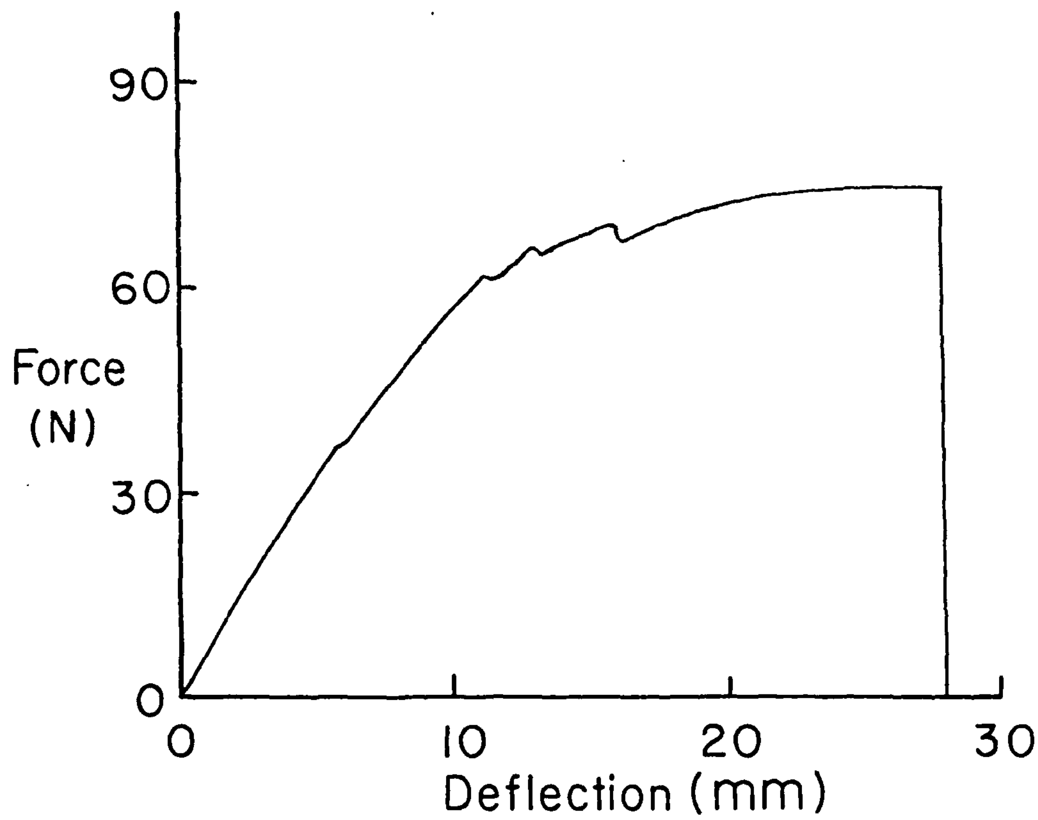

FIG. 3

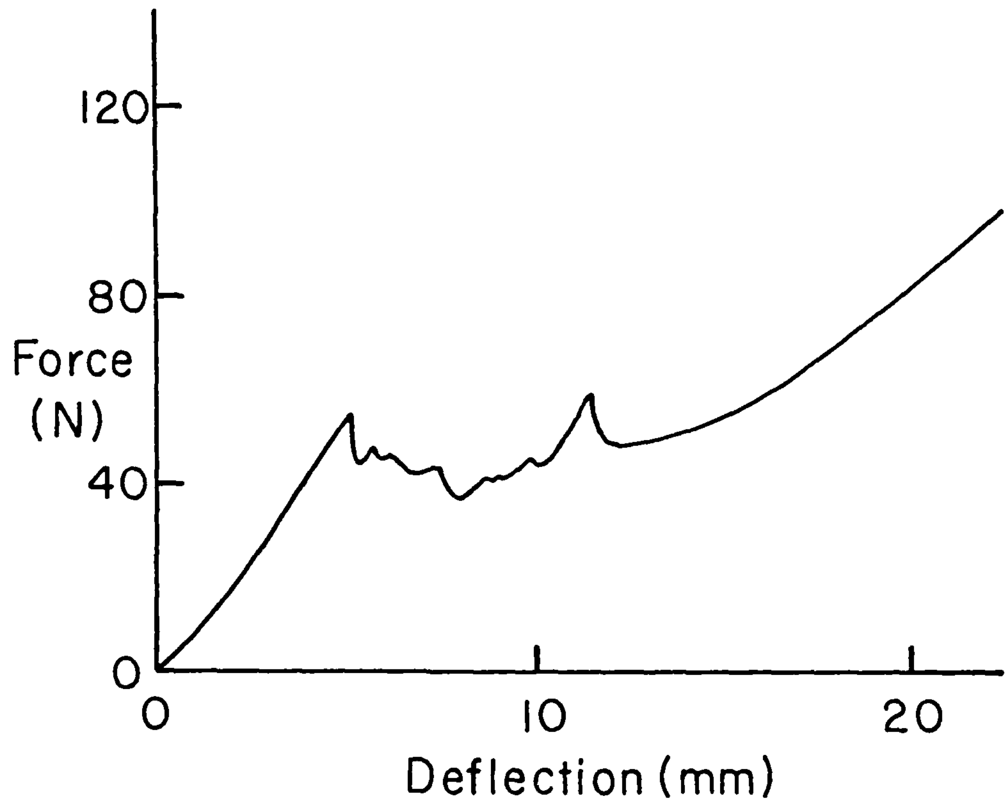

FIG. 4

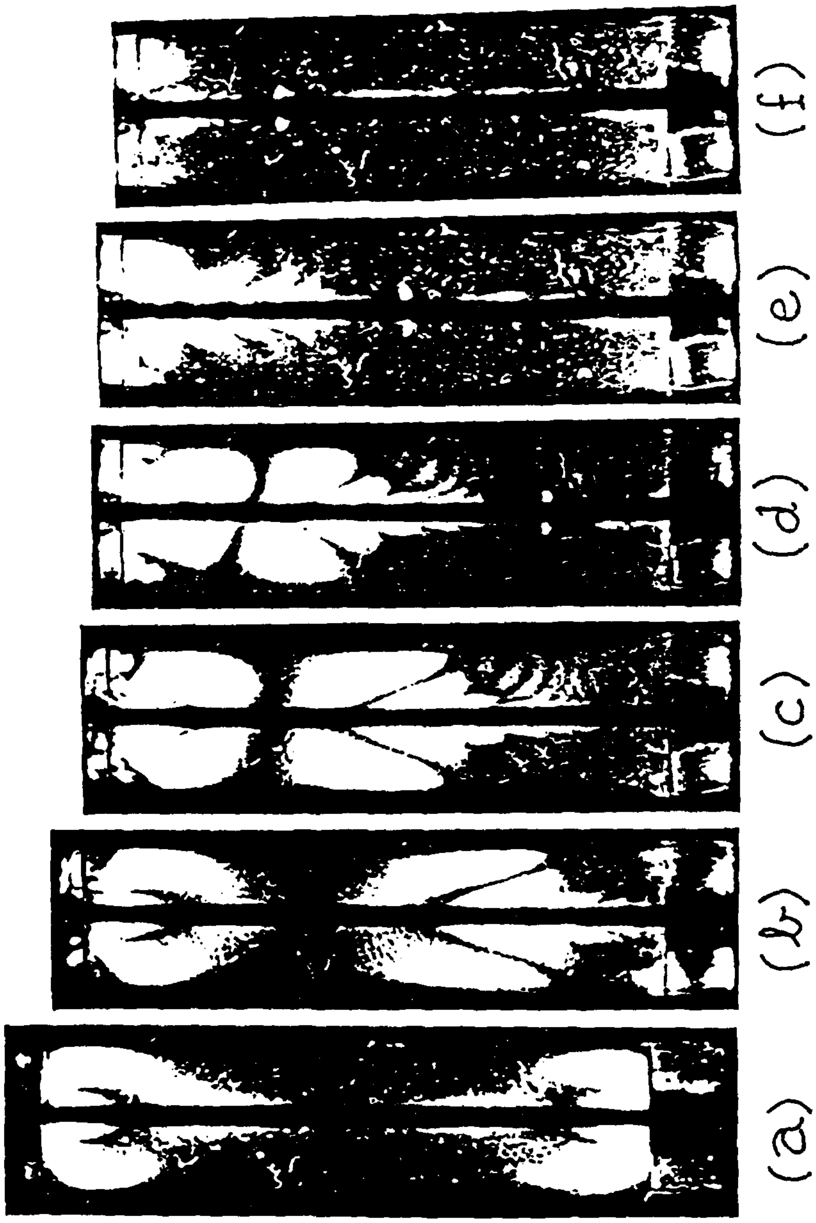

FIG. 5

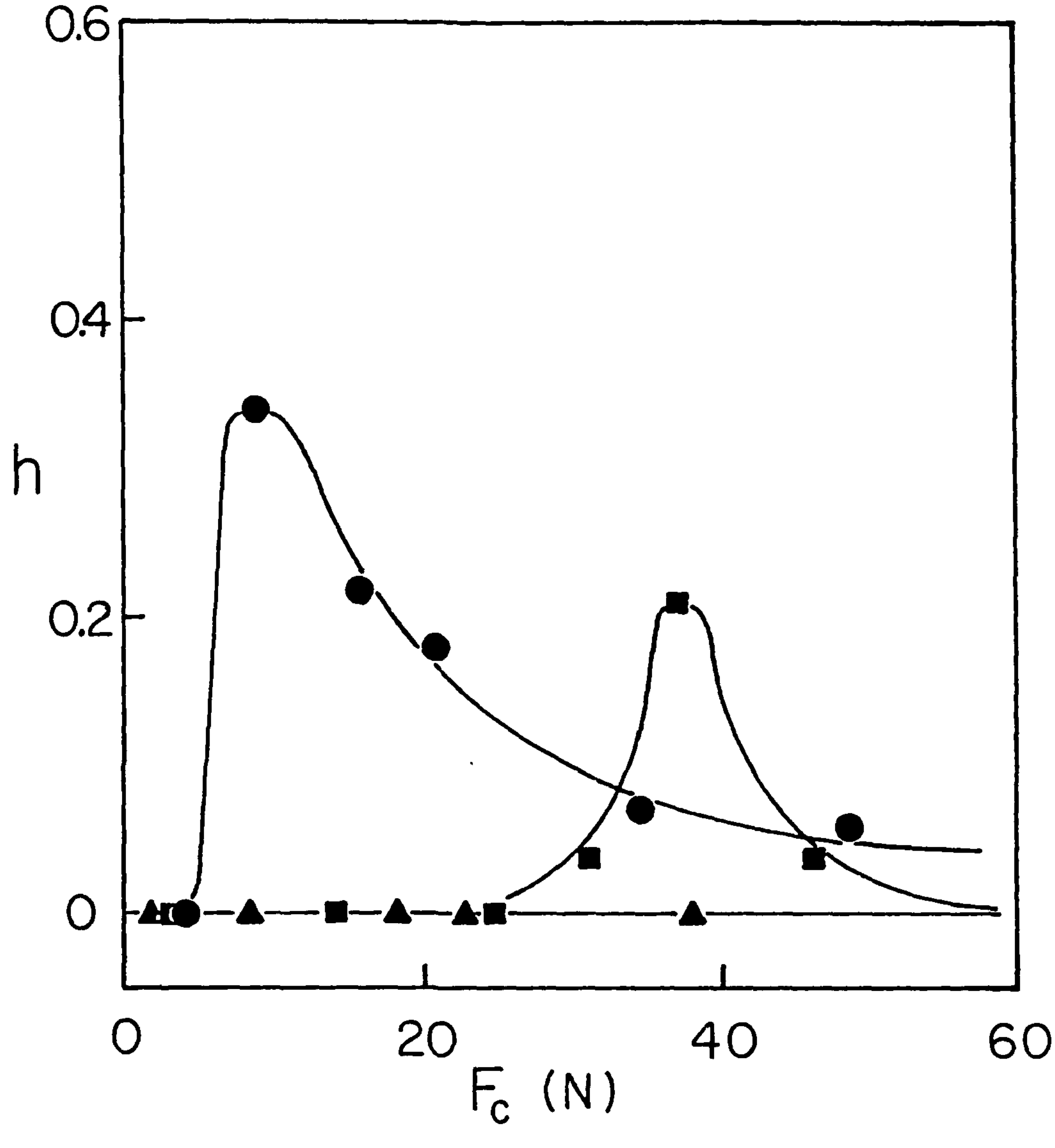

FIG. 6

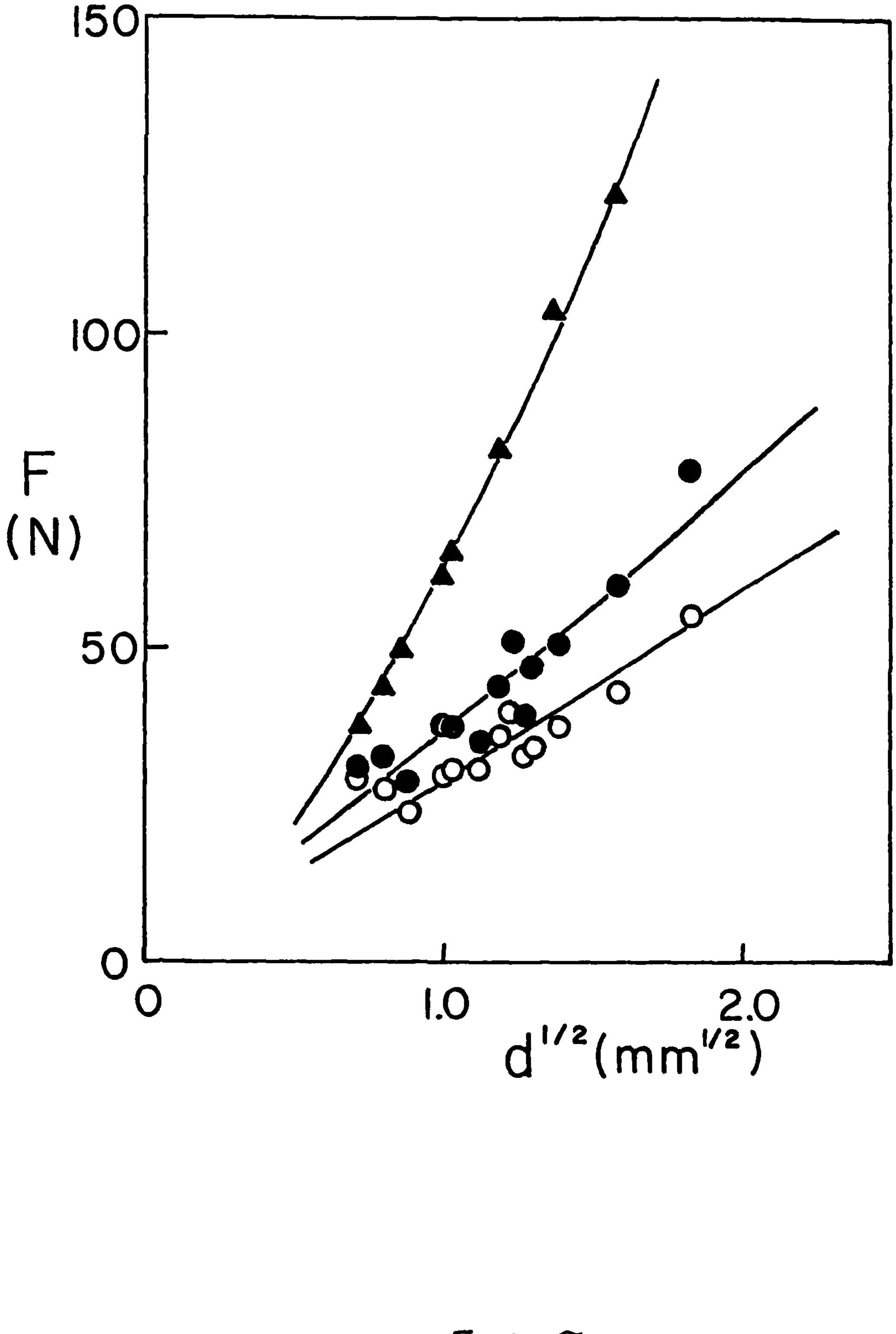

FIG. 7

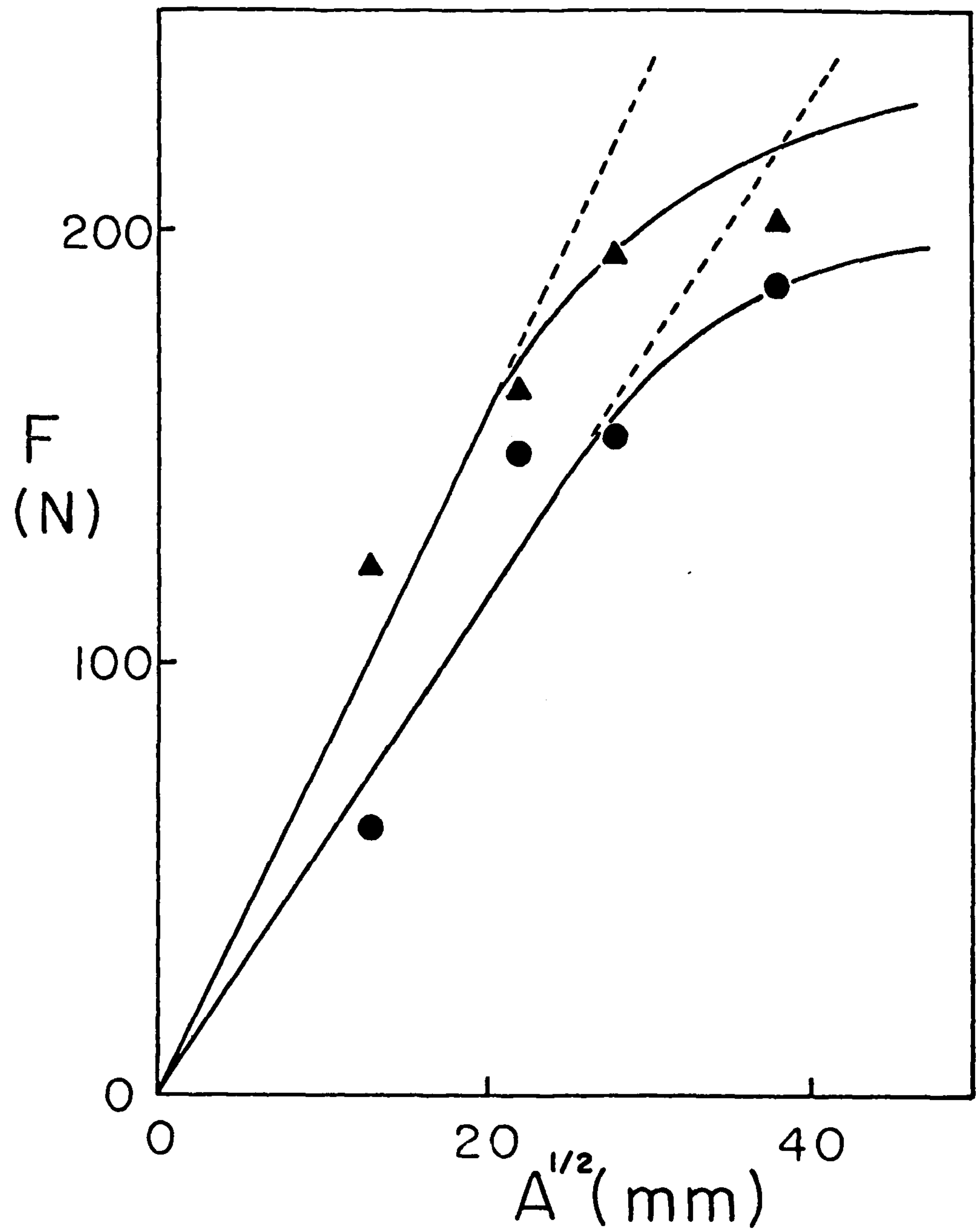

FIG. 8

(DYN)

DISTRIBUTION LIST

Dr. R.S. Miller
Office of Naval Research
Code 432P
Arlington, VA 22217
(10 copies)

Dr. J. Pastine
Naval Sea Systems Command
Code 06R
Washington, DC 20362

Dr. Kenneth D. Hartman
Hercules Aerospace Division
Hercules Incorporated
Alleghany Ballistic Lab
P.O. Box 210
Cumberland, MD 20502

Mr. Otto K. Heiney
AFATL-DLJG
Elgin AFB, FL 32542

Dr. Merrill K. King
Atlantic Research Corp.
5390 Cherokee Avenue
Alexandria, VA 22312

Dr. R.L. Lou
Aerojet Strategic Propulsion Co.
Bldg. 05025 - Dept 5400 - MS 167
P.O. Box 15699C
Sacramenta, CA 95813

Dr. R. Olsen
Aerojet Strategic Propulsion Co.
Bldg. 05025 - Dept 5400 - MS 167
P.O. Box 15699C
Sacramento, CA 95813

Dr. Randy Peters
Aerojet Strategic Propulsion Co.
Bldg. 05025 - Dept 5400 - MS 167
P.O. Box 15699C
Sacramento, CA 95813

Dr. D. Mann
U.S. Army Research Office
Engineering Division
Box 12211
Research Triangle Park, NC 27709-2211

Dr. L.V. Schmidt
Office of Naval Technology
Code 07CT
Arlington, VA 22217

JHU Applied Physics Laboratory
ATTN: CPIA (Mr. T.W. Christian)
Johns Hopkins Rd.
Laurel, MD 20707

Dr. R. McGuire
Lawrence Livermore Laboratory
University of California
Code L-324
Livermore, CA 94550

P.A. Miller
736 Leavenworth Street, #6
San Francisco, CA 94109

Dr. W. Moniz
Naval Research Lab.
Code 6120
Washington, DC 20375

Dr. K.F. Mueller
Naval Surface Weapons Center
Code R11
White Oak
Silver Spring, MD 20910

Prof. M. Nicol
Dept. of Chemistry & Biochemistry
University of California
Los Angeles, CA 90024

Mr. L. Roslund
Naval Surface Weapons Center
Code R10C
White Oak, Silver Spring, MD 20910

Dr. David C. Sayles
Ballistic Missile Defense
Advanced Technology Center
P.O. Box 1500
Huntsville, AL 35807

(DYN)

DISTRIBUTION LIST

Mr. R. Geisler
ATTN: DY/MS-24
AFRPL
Edwards AFB, CA 93523

Naval Air Systems Command
ATTN: Mr. Bertram P. Sobers
NAVAIR-320G
Jefferson Plaza 1, RM 472
Washington, DC 20361

R.B. Steele
Aerojet Strategic Propulsion Co.
P.O. Box 15699C
Sacramento, CA 95813

Mr. M. Stosz
Naval Surface Weapons Center
Code R10B
White Oak
Silver Spring, MD 20910

Mr. E.S. Sutton
Thiokol Corporation
Elkton Division
P.O. Box 241
Elkton, MD 21921

Dr. Grant Thompson
Morton Thiokol, Inc.
Wasatch Division
MS 240 P.O. Box 524
Brigham City, UT 84302

Dr. R.S. Valentini
United Technologies Chemical Systems
P.O. Box 50015
San Jose, CA 95150-0015

Dr. R.F. Walker
Chief, Energetic Materials Division
DRSMC-LCE (D), B-3022
USA ARDC
Dover, NJ 07801

Dr. Janet Wall
Code 012
Director, Research Administration
Naval Postgraduate School
Monterey, CA 93943

Director
US Army Ballistic Research Lab.
ATTN: DRXBR-IBD
Aberdeen Proving Ground, MD 21005

Commander
US Army Missile Command
ATTN: DRSMI-RKL
Walter W. Wharton
Redstone Arsenal, AL 35898

Dr. Ingo W. May
Army Ballistic Research Lab.
ARRADCOM
Code DRXBR - 1BD
Aberdeen Proving Ground, MD 21005

Dr. E. Zimet
Office of Naval Technology
Code 071
Arlington, VA 22217

Dr. Ronald L. Derr
Naval Weapons Center
Code 389
China Lake, CA 93555

T. Boggs
Naval Weapons Center
Code 389
China Lake, CA 93555

Lee C. Estabrook, P.E.
Morton Thiokol, Inc.
P.O. Box 30058
Shreveport, Louisiana 71130

Dr. J.R. West
Morton Thiokol, Inc.
P.O. Box 30058
Shreveport, Louisiana 71130

Dr. D.D. Dillehay
Morton Thiokol, Inc.
Longhorn Division
Marshall, TX 75670

G.T. Bowman
Atlantic Research Corp.
7511 Wellington Road
Gainesville, VA 22065

(DYN)

DISTRIBUTION LIST

R.E. Shenton
Atlantic Research Corp.
7511 Wellington Road
Gainesville, VA 22065

Mike Barnes
Atlantic Research Corp.
7511 Wellington Road
Gainesville, VA 22065

Dr. Lionel Dickinson
Naval Explosive Ordinance
Disposal Tech. Center
Code D
Indian Head, MD 20340

Prof. J.T. Dickinson
Washington State University
Dept. of Physics 4
Pullman, WA 99164-2814

M.H. Miles
Dept. of Physics
Washington State University
Pullman, WA 99164-2814

Dr. T.F. Davidson
Vice President, Technical
Morton Thiokol, Inc.
Aerospace Group
3340 Airport Rd.
Ogden, UT 84405

Mr. J. Consaga
Naval Surface Weapons Center
Code R-16
Indian Head, MD 20640

Naval Sea Systems Command
ATTN: Mr. Charles M. Christensen
NAVSEA-62R2
Crystal Plaza, Bldg. 6, Rm 806
Washington, DC 20362

Mr. R. Beauregard
Naval Sea Systems Command
SEA 64E
Washington, DC 20362

Brian Wheatley
Atlantic Research Corp.
7511 Wellington Road
Gainesville, VA 22065

Mr. G. Edwards
Naval Sea Systems Command
Code 62R32
Washington, DC 20362

C. Dickinson
Naval Surface Weapons Center
White Oak, Code R-13
Silver Spring, MD 20910

Prof. John Deutch
MIT
Department of Chemistry
Cambridge, MA 02139

Dr. E.H. deButts
Hercules Aerospace Co.
P.O. Box 27408
Salt Lake City, UT 84127

David A. Flanigan
Director, Advanced Technology
Morton Thiokol, Inc.
Aerospace Group
3340 Airport Rd.
Ogden, UT 84405

Dr. L.H. Caveny
Air Force Office of Scientific Research
Directorate of Aerospace Sciences
Bolling Air Force Base
Washington, DC 20332

W.G. Roger
Code 5253
Naval Ordance Station
Indian Head, MD 20640

Dr. Donald L. Ball
Air Force Office of Scientific Research
Directorate of Chemical & Atmospheric Sciences
Bolling Air Force Base
Washington, DC 20332

(DYN)

DISTRIBUTION LIST

Dr. Anthony J. Matuszko
Air Force Office of Scientific Research
Directorate of Chemical & Atmospheric
Sciences
Bolling Air Force Base
Washington, DC 20332

Dr. Michael Chaykovsky
Naval Surface Weapons Center
Code R11
White Oak
Silver Spring, MD 20910

J.J. Rocchio
USA Ballistic Research Lab.
Aberdeen Proving Ground, MD 21005-5066

B. Swanson
INC-4 MS C-346
Los Alamos National Laboratory
Los Alamos, New Mexico 87545

Dr. James T. Bryant
Naval Weapons Center
Code 3205B
China Lake, CA 93555

Dr. L. Rothstein
Assistant Director
Naval Explosives Dev. Engineering Dept.
Naval Weapons Station
Yorktown, VA 23691

Dr. M.J. Kamlet
Naval Surface Weapons Center
Code R11
White Oak, Silver Spring, MD 20910

Dr. Henry Webster, III
Manager, Chemical Sciences Branch
ATTN: Code 5063
Crane, IN 47522

Dr. A.L. Slafkosky
Scientific Advisor
Commandant of the Marine Corps
Code RD-1
Washington, DC 20380

Dr. H.G. Adolph
Naval Surface Weapons Center
Code R11
White Oak
Silver Spring, MD 20910

U.S. Army Research Office
Chemical & Biological Sciences
Division
P.O. Box 12211
Research Triangle Park, NC 27709

Dr. John S. Wilkes, Jr.
FJSRL/NC
USAF Academy, CO 80840

Dr. H. Rosenwasser
AIR-320R
Naval Air Systems Command
Washington, DC 20361

Dr. Joyce J. Kaufman
The Johns Hopkins University
Department of Chemistry
Baltimore, MD 21218

Dr. A. Nielsen
Naval Weapons Center
Code 385
China Lake, CA 93555

(DYN)

DISTRIBUTION LIST

K.D. Pae
High Pressure Materials Research Lab.
Rutgers University
P.O. Box 909
Piscataway, NJ 08854

Dr. John K. Dienes
T-3, B216
Los Alamos National Lab.
P.O. Box 1663
Los Alamos, NM 87544

A.N. Gent
Institute Polymer Science
University of Akron
Akron, OH 44325

Dr. D.A. Shockey
SRI International
333 Ravenswood Ave.
Menlo Park, CA 94025

Dr. R.B. Kruse
Morton Thiokol, Inc.
Huntsville Division
Huntsville, AL 35807-7501

G. Butcher
Hercules, Inc.
P.O. Box 98
Magna, UT 84044

W. Waesche
Atlantic Research Corp.
7511 Wellington Road
Gainesville, VA 22065

Dr. R. Bernecker
Naval Surface Weapons Center
Code R13
White Oak
Silver Spring, MD 20910

Prof. Edward Price
Georgia Institute of Tech.
School of Aerospace Engineering
Atlanta, GA 30332

J.A. Birkett
Naval Ordnance Station
Code 5253K
Indian Head, MD 20640

Prof. R.W. Armstrong
University of Maryland
Dept. of Mechanical Engineering
College Park, MD 20742

Herb Richter
Code 385
Naval Weapons Center
China Lake, CA 93555

J.T. Rosenberg
SRI International
333 Ravenswood Ave.
Menlo Park, CA 94025

G.A. Zimmerman
Aeroject Tactical Systems
P.O. Box 13400
Sacramento, CA 95813

Prof. Kenneth Kuo
Pennsylvania State University
Dept. of Mechanical Engineering
University Park, PA 16802

T.L. Boggs
Naval Weapons Center
Code 3891
China Lake, CA 93555

(DYN)

DISTRIBUTION LIST

Dr. C.S. Coffey
Naval Surface Weapons Center
Code R13
White Oak
Silver Spring, MD 20910

D. Curran
SRI International
333 Ravenswood Avenue
Menlo Park, CA 94025

E.L. Throckmorton
Code SP-2731
Strategic Systems Program Office
Crystal Mall #3, RM 1048
Washington, DC 23076

R.G. Rosemeier
Brimrose Corporation
7720 Belair Road
Baltimore, MD 20742

C. Gotzmer
Naval Surface Weapons Center
Code R-11
White Oak
Silver Spring, MD 20910

G.A. Lo
3251 Hanover Street
B204 Lockheed Palo Alto Research Lab
Palto Alto, CA 94304

R.A. Schapery
Civil Engineering Department
Texas A&M University
College Station, TX 77843

Dr. Y. Gupta
Washington State University
Department of Physics
Pullman, WA 99163

J.M. Culver
Strategic Systems Projects Office
SSPO/SP-2731
Crystal Mall #3, RM 1048
Washington, DC 20376

Prof. G.D. Duvall
Washington State University
Department of Physics
Pullman, WA 99163

Dr. E. Martin
Naval Weapons Center
Code 3858
China Lake, CA 93555

Dr. M. Farber
135 W. Maple Avenue
Monnovia, CA 91016

W.L. Elban
Naval Surface Weapons Center
White Oak, Bldg. 343
Silver Spring, MD 20910

Defense Technical Information Center
Bldg. 5, Cameron Station
Alexandria, VA 22314
(12 copies)

Dr. Robert Polvani
National Bureau of Standards
Metallurgy Division
Washington, D.C. 20234

Director
Naval Research Laboratory
Attn: Code 2627
Washington, DC 20375
(6 copies)

Administrative Contracting
Officer (see contract for
address)
(1 copy)